A Tyrosyl Radical in an Irradiated Single Crystal of *N*-Acetyl-L-tyrosine Studied by X-band cw-EPR, High-Frequency EPR, and ENDOR Spectroscopies

Alberto Mezzetti, Anna Lisa Maniero, Marina Brustolon,* and Giovanni Giacometti

Dipartimento di Chimica Fisica "A. Miolati", Università di Padova, Italy

Louis Claude Brunel

National High Magnetic Field Laboratory, Tallahassee, Florida

Received: February 2, 1999; In Final Form: September 9, 1999

γ-ray irradiation of an *N*-acetyl-L-tyrosine single crystal produces three stable radicals (A−C) which have been identified and characterized in their hyperfine coupling (hfc) tensors by using conventional and high-frequency electron paramagnetic resonance (HF-EPR) and X-band electron nuclear double resonance (ENDOR). Radical A is a neutral phenoxyl radical of which the **g**-tensor principal value corresponding with a good approximation to the C−O(H) direction is $g_x = 2.0094 \pm 0.0002$. The comparison with the corresponding values obtained for the similar tyrosyl radicals playing a role in different biological systems supports the idea of using the g_x value as a probe to find the presence of a hydrogen-bond interaction involving the phenoxyl oxygen. Radical B is a neutral cyclohexadienyl radical obtained by hydrogen atom addition at a position ortho to the phenolic group of the tyrosine moiety. Its hfc tensors have been fully characterized and found to be in agreement with present theories. Radical C is found to be produced by reduction of the carboxylic group of the parent tyrosine derivative.

Introduction

The tyrosyl radical is a phenoxyl radical obtained as product of the monoelectronic oxidation of tyrosine. It is known to have an important role in some biological systems. In the reaction center (RC) of the photosystem II (PSII) of plants, algae, and cyanobacteria, two tyrosyl radicals have been detected[1] and their function has been thoroughly investigated,[2−8] Tyrosyl radicals have been identified also in ribonucleotide reductase (RNR)[9] and prostaglandine-*H*-syntase.[10]

The magnetic parameters such as the **g** and the hyperfine coupling (hfc) tensors obtained by electron paramagnetic resonance (EPR) spectra of tyrosyl radicals in biological systems have been correlated to their proteic environment. In particular, a correlation has been found between the strength of the H-bond formed by the tyrosine phenoxyl oxygen with the surrounding molecules and the **g** tensor principal values.[11] Moreover, the hfc tensors are important to trace a spin density map of the radical, which some authors believe to be environment-dependent.[12]

The characterization by EPR of a model system containing a tyrosyl radical in a precisely known environment and orientation is of some interest as it can help in interpreting the data collected for biological systems.

Tyrosyl radicals in γ-irradiated L-tyrosine hydrochloride (L-tyr-HCl) single crystals have been studied by Fassanella and Gordy[13] and by Box and co-workers.[14] In addition, frozen[15−18] and fluid solutions[19,20] of the same radicals were studied. A drawback of the single-crystal model is that L-tyr-HCl crystallizes in ionic form. Moreover, the study by King et al.,[13] which is usually taken as a reference point by modern authors, has been carried out by using uniquely X-band cw-EPR spectroscopy, which is not sufficient to measure precisely **g** and hfc tensors of radicals in solid samples.

In this paper, we report a detailed X-band cw-EPR, high-frequency EPR (HF-EPR) and ENDOR (electron nuclear double resonance) study on the tyrosyl radical produced by γ-irradiation on a single crystal of *N*-acetyl-L-tyrosine.

Experimental Section

Single crystals of *N*-acetyl-L-tyrosine were obtained by slow evaporation at room temperature of a water solution. *N*-Acetyl-L-tyrosine crystallizes in the monoclinic space group $P2_1$, with cell parameters $a = 5.994$, $b = 7.495$, and $c = 12.510$ Å, $\beta = 101.77°$, and $Z = 2$.[21] The crystals were irradiated at room temperature by γ-rays from a ^{60}Co source with a dose of 3 Mrad.

X-band cw-EPR spectra were recorded at a frequency of 9.4 GHz using a conventional Bruker ER200D spectrometer interfaced with a Bruker data system ESP1600 and equipped with a Bruker variable temperature unit.

ENDOR spectra were obtained by using a Bruker ER200 D spectrometer with a Bruker TM_{110} cavity containing a radio frequency (RF) coil. The RF is generated by a Rohde & Schwarz SMX synthesizer and swept in the proton frequency range by a computer that also provides for the data acquisition. The RF is frequency-modulated with 25 kHz by using a EG & G 5208 lock-in, and the ENDOR signal is recorded as the first derivative. Amplification of the frequency-modulated RF is achieved with an ENI A-300 amplifier.

ENDOR spectra were recorded at the temperature of 240 K in the three crystallographic planes every 6°. For this purpose, a single crystal was mounted on a goniometer rod and rotated in the ENDOR cavity around the three crystallographic axes: *a*, *b*, and *c**.

* Department of Physical Chemistry "A.Miolati", University of Padova, Via Loredan, 2, I-35100 Padova. E-mail: m.brustolon@chfi.unipd.it. Fax: +39−049−8275135.

10.1021/jp9903763 CCC: $18.00
Published on Web 11/12/1999

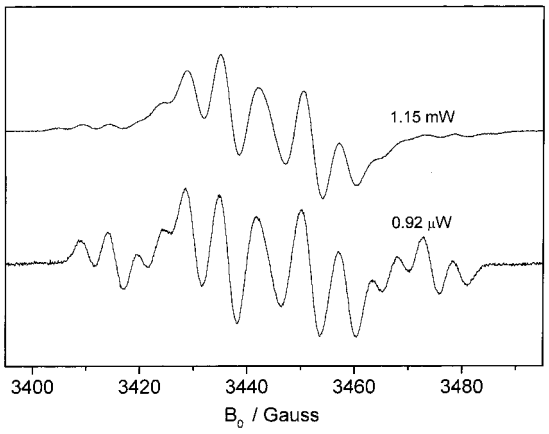

Figure 1. X-band EPR spectra of an *N*-acetyl-L-tyrosine single crystal for a casual orientation of the crystal at two different microwave powers.

High-frequency EPR spectra were recorded at the high-field electron magnetic resonance facility of the National High Magnetic Field Laboratory in Tallahassee, Florida. The EPR spectrometer has a design similar to the instrument described by Mueller et al.,[22] except for the following modifications: the sources are Gunn diodes oscillators (from Abmm, Paris), equipped with Schottky diode harmonic generators; the magnetic field is provided by a 15/17 T (at 4.2 and 2.2 K, respectively) superconducting Oxford Instruments magnet, and the detector is a "hot electron" InSb bolometer (from QMC, London). The spectra are recorded in the magnetic field first-derivative mode.

Results

X-band cw-EPR. Because of the monoclinic crystal structure of *N*-acetyl-L-tyrosine, two magnetically nonequivalent sites are present. Therefore, for any orientation of the crystal in the magnetic field, the spectrum is given by the superposition of the spectra due to the radicals in the two sites.

However, when the magnetic field is along a crystallographic axis or when it is in the crystallographic plane perpendicular to the *b* axis, the two sites become magnetically equivalent. The pronounced asymmetry of the spectra also for these latter orientations indicates the superposition of signals due to different radicals with different **g** tensors.

All of the spectra obtained showed two quite distinguishable groups of lines: an intense multiplet in a range of about 40 G surrounded at the wings by some other lines of minor intensity. On varying the microwave power, a different behavior can be noticed for the two groups of lines, with the outer ones saturating at lower power with respect to the inner ones, as shown in Figure 1. On this evidence, we concluded that the spectrum is given at least by two different radicals. We will call radical A the one giving rise to the internal multiplet, and radical B the other one.

Because of the complexity of the spectra, we did not try a full analysis by rotating the crystal around the three crystallographic axes and, for this kind of study, switched to the ENDOR spectroscopy.

ENDOR. We will consider in the following only proton ENDOR transitions. We will call high-frequency ENDOR transitions ν_+ those given by $\nu_+ = |A/2| + \nu_H$, where A is approximately the hyperfine splitting and ν_H is the free proton frequency, and low-frequency ENDOR transitions ν_- the ones given by $\nu_- = ||A/2| - \nu_H|$. Depending on the positive or negative sign of the hyperfine coupling, the lines at frequency (ν_+, ν_-) will correspond respectively to the ($m_s = -1/2$, $m_s = +1/2$) or to the ($m_s = +1/2$, $m_s = -1/2$) electron spin manifolds.

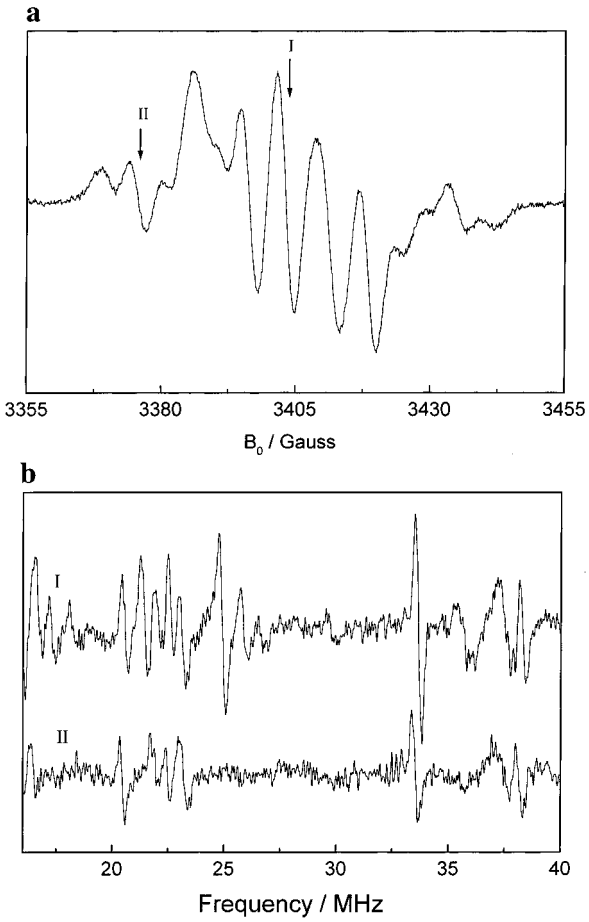

Figure 2. (a) X-band EPR spectrum of an *N*-acetyl-L-tyrosine single crystal oriented with the magnetic field at an angle of 24° from the *b* axis. (b) ENDOR spectra of the same sample and orientation as in part a, with magnetic field on the two positions shown by the arrows in part a.

The ENDOR investigation has been done in the frequency interval 16−40 MHz, and the angular dependences of the ν_+ frequencies have been followed.

The measured ENDOR frequencies for any orientation of the crystal in the magnetic field depend on the irradiated EPR hyperfine component. We recorded two series of ENDOR spectra with the magnetic field fixed, respectively, on the EPR external lines (radical B) and on the internal ones (radical A + radical B). In Figure 2 the EPR spectrum for the magnetic field placed in the *bc** plane at an angle of 24° from the *b* axis is shown, together with the ENDOR spectra observed on the two marked positions. The angular dependences of the ENDOR frequencies have been fitted by the usual first-order analysis.[23] In Figure 3, the best fitting curves corresponding to a rotation around the *a* axis are reported.

From the angular dependences of the frequencies for rotations around the crystallographic axes, we have obtained the hfc tensors reported in Tables 1 and 2.

The attribution of the hfc tensors to protons belonging to the two radicals was made by assuming that the ENDOR frequencies observed only on the external EPR lines must belong to radical B, whereas those observed on the internal EPR lines must be due to both radicals A and B. However, a pair of symmetry-related broad high-frequency ENDOR lines observed on the internal multiplet that can be followed in the three rotation planes cannot be attributed to either radical A or B, because the width of the EPR spectrum and number of lines would not match with the experimentally observed ones.

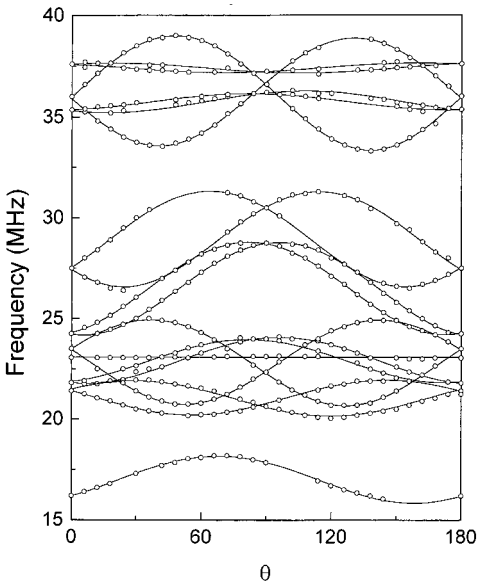

Figure 3. Experimental ENDOR frequencies (±0.1 MHz) and best-fitting curves obtained while rotating the crystal around the *a* axis.

TABLE 1: Experimental Hyperfine Coupling Tensors and Calculated Dipolar Tensors for Radical A

	isotropic constant (MHz)	principal dipolar values (MHz)	direction cosines between principal and crystal axes		
			a	*b*	*c**
A_1 proton	−19.7 ± 0.3	10.7 ± 0.3	−0.8827	−0.4597	0.0972
		−9.2 ± 0.3	0.1997	−0.1798	0.9632
		−1.5 ± 0.3	0.4253	−0.8696	0.2505
C(3) proton (calculated)		8.5	−0.9146	−0.4009	0.0531
		−6.8	0.0183	−0.1932	0.9810
		−1.7	0.4041	−0.8956	0.1859
A2 proton	−17.5 ± 0.3	9.3 ± 0.3	0.4700	0.3987	0.7870
		−8.0 ± 0.3	0.7876	0.2132	−0.5786
		−1.3 ± 0.3	0.3984	−0.8919	0.2137
C(5) proton (calculated)		8.5	0.5656	0.4025	0.7198
		−6.8	0.7143	0.1830	−0.6755
		−1.7	0.4041	−0.8956	0.1859
A_3 proton	5.4 ± 0.3	2.4 ± 0.3	−0.8685	−0.4660	0.1691
		1.6 ± 0.3	0.2937	−0.2089	0.9328
		−4.0 ± 0.3	0.3994	−0.8597	−0.3183
C(6) proton (calculated)		2.8	−0.9148	−0.3945	0.0985
		0.8	0.0157	0.2090	0.9778
		−3.7	0.4038	−0.8959	0.1850
A_4 proton	43.3 ± 0.3	3.7 ± 0.3	0.8190	−0.2366	−0.5225
		−1.2 ± 0.3	0.4553	0.8222	0.3412
		−2.5 ± 0.3	−0.3489	0.5174	−0.7813
β proton (calculated)		5.1	0.3152	−0.5135	−0.8192
		−2.3	0.5304	0.7954	0.2932
		−2.8	−0.7796	0.3275	−0.5340

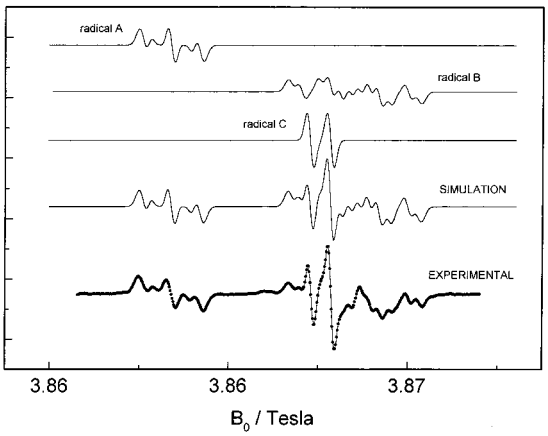

Figure 4. HF-EPR spectra of a single crystal of *N*-acetyl-L-tyrosine recorded with the magnetic field parallel to the *c** axis together with its simulation. The contributions of the three radicals A−C (see text) to the simulated spectrum are also shown.

We must therefore attribute this hfc tensor to a proton belonging to a third radical, radical C.

A test of the consistency of the previous analysis is given by the simulations of the HF−EPR spectra, reported in the following paragraph.

High-Frequency EPR. HF−EPR spectra have been recorded at a frequency of about 108 GHz. The exact value of the frequency has been changed several times from a measurement to another one to reach the best possible signal-to-noise ratio. The crystal was rotated around the three principal axes, *a*, *b*, and *c**; spectra were recorded every 4.5° of each rotation.

The interpretation of the spectra recorded with the magnetic field perpendicular to the binary axis was easy because in a large angular portion during the rotation there was a separation between the signals arising from radicals B and C, and the signal arising from radical A.

The signal arising from any of the three radicals A−C can be simulated using the hyperfine coupling values found for the same orientation with the ENDOR analysis and an adequate value for the *g* factor. From the superposition of the three simulated spectra of each single radical, it was finally possible to simulate the overall spectrum.

Good simulations were obtained only for the spectra recorded with the static magnetic field perpendicular to the binary axis or parallel to each of the *a*, *b*, and *c** crystallographic axes, as in these orientations the two sites present in the crystals become magnetically equivalent, leading to a simpler overall spectrum. For other orientations, the spectra are the result of six different signals that are almost impossible to identify. This fact did not allow us to measure completely the **g** tensors for the three radicals.

In Figure 4, the experimental spectrum recorded with the static magnetic field parallel to the *c** axis is shown together with its simulation.

TABLE 2: π Spin Density Distribution for Different Tyrosyl Radicals

	RNR[a] *Escherichia coli*	PSII Y_D•[a]	PSII Y_Z•[a]	frozen solution[a]	frozen solution[b]	SCF calcd[c]
O	0.29 ± 0.02	0.26 ± 0.02[d]	0.26 ± 0.02	0.26 ± 0.02	0.26 ± 0.01	0.26
C_1	0.38 ± 0.02	0.37 ± 0.02	0.37 ± 0.02	0.34 ± 0.02	0.32 ± 0.01	0.31
$C_{2,C6}$	−0.08 ± 0.02	−0.07 ± 0.02	−0.07 ± 0.02	−0.07 ± 0.02	−0.04 ± 0.01	−0.045
$C_{3,C5}$	0.25 ± 0.02	0.24 ± 0.02	0.26 ± 0.02	0.24 ± 0.02	0.23 ± 0.01	0.26
C_4	−0.05 ± 0.02[e]	0.01 ± 0.02[e]	−0.01 ± 0.02[e]	0.02 ± 0.02[e]	−0.01 ± 0.01	−0.03
$C_{methylene}$	0.03 ± 0.02	0.01 ± 0.02	-	-	-	-

[a] Hoganson et al.[9] [b] Hulsebosch et al.[16] [c] Fassanella and Gordy.[13] [d] ^{17}O experiments[8] have shown that the π spin density on the oxygen atom is 0.28 ± 0.01. [e] For C_4, Hoganson et al.[9] suggest that the error can be larger than ±0.02.

SCHEME 1

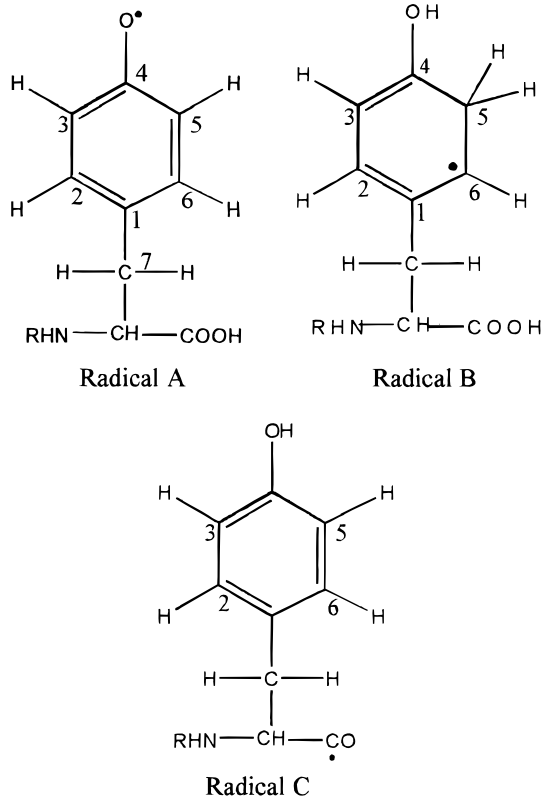

Discussion

The HF-EPR spectrum for B//c^* (Figure 4) shows clearly the presence of the three radicals *A*−C.

Radical A. On the basis of the comparison of our results with those derived from different studies on the tyrosyl radical,[3−20] and in particular with that on γ-irradiated L-tyrosine hydrochloride,[13] we identify radical A with the phenoxyl radical reported in Scheme 1.

We suggest that the phenolic hydrogen atom of an *N*-acetyl-L-tyrosine on formation of such a radical is lost to another molecule, not necessarily a neighboring one, to form a reduction product (see radicals B and C).

The attribution of the tensors in Table 1 to the different protons was made by comparing the experimental results with the dipolar tensors calculated by the McConnell−Strathdee (M−S) method.[24] For the calculation, we used the atomic coordinates obtained from the crystal structure[21] and a spin density distribution obtained with a self-consistent field (SCF) procedure:[13] ($\rho(C_1) = 0.31$, $\rho(C_2) = \rho(C_6) = -0.045$, $\rho(C_4) = -0.03$, $\rho(C_3) = \rho(C_5) = 0.26$, $\rho(O) = 0.28$.). This spin distribution is consistent with recent comprehensive analyses on in vivo[8,9] and in vitro[16,17] tyrosyl radicals (see Table 2). It may be added that this spin distribution, within the indicated small range of variation, can be considered typical of alkyl-substituted phenoxyl radicals, irrespective of the detailed alkyl substituent to ring carbons; for example, see earlier studies.[25−28]

First of all, we attributed to the ring protons at positions 3 and 5 the two hfc tensors with the largest dipolar contribution (tensors $\mathbf{A}_1$ and $\mathbf{A}_2$). The tensors are reported in Table 1. The agreement between both the principal values and principal axes directions of the hfc tensors is good enough to consider the attribution a safe one. It should be noted that the two protons have slightly different principal values of the hfc tensors, indicating that the molecular axis C(1)−C(4) is not a symmetry axis for the spin distribution.

The hfc tensor with the smallest principal values (tensor $\mathbf{A}_3$) has been attributed to proton C(6)−H. In addition, in this case, the attribution is checked by the calculated tensor reported in Table 1. It should be noted that in this case the carbon atom 6 is bearing a negative spin density due to spin polarization of the π electrons, as obtained by the calculated values, giving rise to a positive isotropic hfc constant.

The hfc tensor of proton C(2)−H has not been determined due to the overlap of its ENDOR lines with those of the matrix protons.

The hfc tensor with the largest isotropic hfc constant (tensor $\mathbf{A}_4$) has been attributed to one of the methylene β-protons. Let us call $H_{\beta 1}$ the proton corresponding to tensor $\mathbf{A}_4$, and $H_{\beta 2}$ the other β-proton. The well-known semiempirical expression:[23]

$$A_H^{\beta} = B \cos^2 \theta \, \rho^{\pi}_C \qquad (1)$$

links the isotropic hfc constant A_H^{β}, the semiempirical parameter *B*, the π spin density ρ^{π}_C on carbon atom 1, and the dihedral angle θ defined by the methylene group carbon−proton bond, C_1, and the normal to the ring.

We can obtain an estimated value for the angle θ by comparing the constant A_H^{β} with the corresponding one measured for a similar phenoxyl radical bearing a methyl group in a position para to the C−O bond. In fact, this kind of comparison can be safely made because it is known that all of the phenoxyl radicals have very similar molecular properties.[25] We may then safely compare the results for tyrosyl radical with those for the radical 4-methyl-2,6-di-*tert*-butylphenoxyl. The isotropic hfc constant of the methyl group protons of the latter radical is $A^{\beta}_{CH_3} = 31.5$ MHz,[28] and taking into account that $\langle \cos^2 \theta \rangle = 0.5$ for a rotating methyl group, from eq 1, we obtain $B\rho^{\pi}_C = 63$ MHz. By assuming a constant value of the quantity $B\rho^{\pi}_C$ for different phenoxyl radicals, from the comparison of their isotropic hfc constants A_H^{β}, it is possible to get information on the orientation of the C(7)−H_{β} bonds with respect to the phenoxyl ring. From the value $A_H^{\beta} = 43.3$ MHz, a dihedral angle $\theta_1 = 34°$ is obtained between the C(7)−$H_{\beta 1}$ bond and the axis of the π orbital on the phenoxyl ring of radical A. On the other hand, because the isotropic hfc constant of the other β-proton must be very small because it is not detectable in the ENDOR and EPR spectra, the corresponding dihedral angle formed by the C(7)−$H_{\beta 2}$ bond must be $\theta_2 \approx 90°$.

These values can be compared with the dihedral angles defined by the two C(7)−H bonds, C_1 and the direction perpendicular to the phenolic ring in the undamaged molecule. From the coordinates of the crystal structure, we obtain for the two latter angles the values of 30° and 90°, respectively. Therefore, we can conclude that the conformation of the radical and that of the undamaged molecule are nearly the same. The HF-EPR spectra allowed us to determine the angular dependence of the *g* anisotropy in the $a-c^*$ crystallographic plane.

From the crystallographic structure, we know that the tyrosine ring is in the $a-c^*$ plane and the C−OH bond forms an angle of 26° with the c^* axis. On the other hand, we know from the comparison of all of the calculated principal directions of the dipolar coupling tensors with the experimental ones that the radical occupies in the crystal structure the same position as the undamaged molecule. Therefore, from the data in Figure 5, we can get the value of the *g* factor for B parallel to the C−O direction. This value should correspond with a good approximation to the maximum principal value g_{max} of the **g** tensor.[11]

In Figure 5, we have indicated with an arrow the angle corresponding to the C−O bond direction, and it can be noted

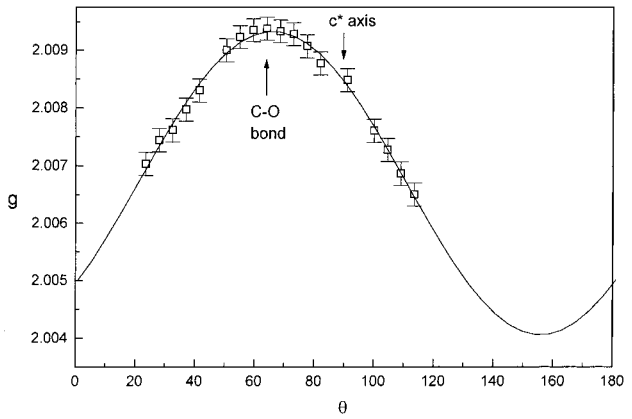

Figure 5. g values for the tyrosyl radical (radical A) on rotation in the $a-c^*$ plane. The direction parallel to the C−O bond is indicated by an arrow.

TABLE 3: Hyperfine Coupling Tensors for Radical B

	isotropic constant (MHz)	principal dipolar values (MHz)	direction cosines between principal and experimental axes		
			a	*b*	*c**
B_1 proton[a]	78.0 ± 0.3	5.7 ± 0.3	0.9785	0.1928	−0.0719
		−2.9 ± 0.3	0.2019	−0.9670	0.1547
		−2.8 ± 0.3	−0.0397	−0.1660	−0.9853
B_2 proton[a]	47.4 ± 0.3	5.2 ± 0.3	0.8929	0.4341	−0.1187
		−3.4 ± 0.3	0.4493	−0.8748	0.1807
		−1.8 ± 0.3	−0.0254	−0.2147	−0.9763
B_3 proton[b]	−46.3 ± 0.3	22.0 ± 0.3	0.5368	−0.2773	−0.7967
		−24.9 ± 0.3	0.8108	−0.0911	0.5780
		3.0 ± 0.3	−0.2329	−0.9564	0.1760
B_4 proton[c]	−14.2 ± 0.3	6.3 ± 0.3	0.9246	−0.3677	0.2303
		−5.1 ± 0.3	0.1752	0.1794	0.9680
		−1.2 ± 0.3	−0.3382	−0.9124	−0.0991
B_5 proton[d]	12.5 ± 0.3	3.9 ± 0.3	0.6659	0.1372	0.7332
		−5.7 ± 0.3	0.6867	0.2710	−0.6744
		1.9 ± 0.3	−0.2412	0.9527	0.0862

[a] Attributed to C(5) proton; see Scheme 1. [b] Attributed to C(2) proton. [c] Attributed to C(6) proton. [d] Attributed to C(3) proton. Signs of hfc constant and principal values of dipolar tensor are taken for a negative spin density; see text.

that it corresponds really to the maximum value of the g angular dependence. We get $g_{max} = 2.0094 \pm 0.0002$.

In a later section, we will discuss this value as compared with the corresponding values obtained for the tyrosyl radical in other systems, in particular the biological ones.

Radical B. We attribute to radical B the structure reported in Scheme 1. It is known that radicals of this type are formed in L-tyrosine and poly-L-tyrosine powder samples irradiated with γ-rays or bombarded with H atoms.[29,28]

In Table 3, we report the five hfc tensors determined for this radical. The structure of the first two dipolar tensors $\mathbf{B}_1$ and $\mathbf{B}_2$, nearly axial, indicate two β-protons, whereas tensors $\mathbf{B}_3-\mathbf{B}_5$ have structures typical of α-protons (a, $-a$, 0).

The hypothesis that the two β-protons are attached to C(5) can be supported by comparing the C(5)−H direction in the undamaged crystal structure with the principal directions corresponding to the largest principal values of the two tensors. In fact, the latter principal directions should correspond approximately to those of the two C(5)−H bonds in the radical. Therefore, the direction bisecting the H−C(5)−H angle in the radical should be approximately parallel to the direction of the C(5)−H bond in the undamaged crystal. We find an angle of 7° between these two directions.

TABLE 4: Hyperfine Coupling Tensor for Radical C

	isotropic constant (MHz)	principal dipolar values (MHz)	direction cosines between principal and experimental axes		
			a	*b*	*c**
C_1 proton	28.0 ± 0.3	8.0 ± 0.3	0.4561	0.3876	0.8011
		−3.5 ± 0.3	0.5351	0.5998	−0.5949
		−4.5 ± 0.3	−0.7110	0.7000	0.0661

By starting from the attribution of tensors $\mathbf{B}_1$ and $\mathbf{B}_2$ to the protons attached to C(5), we can attribute tensors $\mathbf{B}_3$, $\mathbf{B}_4$, and $\mathbf{B}_5$ to the α-H attached to carbon atoms C(2), C(6), and C(3), respectively. This attribution is done by comparing the isotropic hfc constants for the present radical with those for a cyclohexadienyl radical.[31] We have checked the attribution of tensor $\mathbf{B}_4$ in Table 3 to the C(6)−H proton on the basis of the following considerations. When a substantial spin density is present on a carbon atom belonging to a π radical system, the principal direction of the largest positive principal value of the corresponding $C-H_\alpha$ proton hfc tensor will be approximately parallel to the $C-H_\alpha$ bond.[23] If we compare the latter principal directions for tensors $\mathbf{B}_4$ and $\mathbf{A}_1$ (see Tables 3 and 1), we see that the two directions are nearly parallel as expected, because the C(3)−H and C(6)−H bonds should have the same directions (see Scheme 1).

It should be noted that in Table 3 we have ascribed a positive sign to the isotropic hfc constant attributed to the C(3)−H proton (tensor $\mathbf{B}_3$), because for a cyclohexadienyl radical a negative spin density is expected on carbon atoms C(1) and C(3), due to the spin polarization of the π electrons.[31]

Radical C. The third radical presents only one hfc tensor (see Table 4). The value of the isotropic hfc constant and the structure of the dipolar tensor indicate a β proton. A possible structure for this radical is reported in Scheme 1.

This kind of radical, produced by reduction of the carboxylic group, has been identified in irradiated crystals of carboxylic acids.[32]

Comparison with Tyrosyl Radicals in Photosynthetic Systems. The two tyrosyl radicals detected in PSII are generated by the action of the oxidizing species P680+, the photogenerated cation of the primary donor. One of these, called Y_Z•, is a transient radical because it is soon reduced by the oxygen evolving complex (OEC), whereas the other, called Y_D•, is stable in the oxidized state for hours.

Both radicals take part, as acceptor partners, in a hydrogen bond,[31] although in the case of Y_Z• the hydrogen bond does not seem to be well-defined. The different redox behavior of the two tyrosine molecules is probably also related to the different characteristics of the environment (hydrophobic for Y_Z•, hydrophilic for Y_Z•),[32,33] to their mobility (large for Y_Z• and poor for Y_D•),[3,34] and to the different disposition in the structure of the RC (Y_Z• seems to be closer to the OEC than Y_D•).[35]

All of these results have suggested[3] that the two tyrosine residues play a completely different role in the RC. According to this model, the Y_D tyrosine seems to be involved in a simple electron-transfer process; in the reduced state, its phenolic proton is hydrogen-bonded to a nearby histidine, whereas upon oxidation, the proton is retained in the site and the sense of the hydrogen-bond interaction is reversed. This ensures a minimization of the nuclear motion, as required by an efficient electron transfer according to the Marcus theory.

The role of Y_Z tyrosine seems to be different. As for Y_D, it has been postulated that in the oxidized state Y_Z• there is a hydrogen-bond interaction between the phenoxyl oxygen and a

TABLE 5: Hyperfine Coupling Tensors for Tyrosyl Radicals in Different Systems[a]

position	*N*-ac-L-tyr[b] (crystals)	L-tyr-HCl[c] (crystals)	RNR[d] *Escherichia coli*	PSII Y_D•[e] *Synechocystis* 6803	PS II Y_Z•[f] *Synechocystis* 6803
ring 3	$A_i = -19.7 \pm 0.3$ $T_x = 10.7 \pm 0.3$ $T_y = -9.2 \pm 0.3$ $T_z = -1.5 \pm 0.3$	$A_i = -17.4 \pm 1.4$ $T_x = 8.7 \pm 1.4$ $T_y = -7.8 \pm 1.4$ $T_z = -0.8 \pm 1.4$	$A_i = -18{,}2 \pm 0.1$ $T_x = -8.5 \pm 0.1$ $T_y = 9.8 \pm 0.1$ $T_z = -1.4 \pm 0.1$	$A_i = -17.4 \pm 0.3$ $T_x = 10.2 \pm 0.3$ $T_y = -8.0 \pm 0.3$ $T_z = -2.1 \pm 0.3$	$A_i = -18.2 \pm 0.3$ $T_x = 9.8 \pm 0.3$ $T_y = -8.6 \pm 0.3$ $T_z = -1.3 \pm 0.3$
ring 5	$A_i = -17.5 \pm 0.3$ $T_x = 9.3 \pm 0.3$ $T_y = -8.0 \pm 0.3$ $T_z = -1.3 \pm 0.3$	$A_i = -17.4 \pm 1.4$ $T_x = 8.7 \pm 1.4$ $T_y = -7.8 \pm 1.4$ $T_z = -0.8 \pm 1.4$	$A_i = -18{,}2 \pm 0.1$ $T_x = 9.8 \pm 0.1$ $T_y = -8.5 \pm 0.1$ $T_z = -1.4 \pm 0.1$	$A_i = -17.4 \pm 0.3$ $T_x = 10.2 \pm 0.3$ $T_y = -8.0 \pm 0.3$ $T_z = -2.1 \pm 0.3$	$A_i = -18.2 \pm 0.3$ $T_x = 9.8 \pm 0.3$ $T_y = -8.6 \pm 0.3$ $T_z = -1.3 \pm 0.3$
ring 2	*g*	*g*	$A_i = 4.9 \pm 0.1$ $T_x = 2.7 \pm 0.1$ $T_y = 0.2 \pm 0.1$ $T_z = -2.8 \pm 0.1$	*g*	$A_i = 4.6 \pm 0.3$ $T_x = 2.9 \pm 0.3$ $T_y = 0.4 \pm 0.3$ $T_z = -3.3 \pm 0.3$
ring 6	$A_i = 5.4 \pm 0.3$ $T_x = 2.4 \pm 0.3$ $T_y = 1.6 \pm 0.3$ $T_z = -4.0 \pm 0.3$	*g*	$A_i = 4.9 \pm 0.1$ $T_x = 2.7 \pm 0.1$ $T_y = 0.2 \pm 0.1$ $T_z = -2.8 \pm 0.1$	*g*	$A_i = 4.6 \pm 0.3$ $T_x = 2.9 \pm 0.3$ $T_y = 0.4 \pm 0.3$ $T_z = -3.3 \pm 0.3$
methylene	$A_i = 43.3 \pm 0.3$ $T_x = 3.7 \pm 0.3$ $T_y = -1.2 \pm 0.3$ $T_z = -2.5 \pm 0.3$	$A_i = 39.2 \pm 1.4$ $T_x = 0$ $T_y = 0$ $T_z = 0$	$A_i = 56.2 \pm 0.1$ $T_x = 5.0 \pm 0.1$ $T_y = -2.5 \pm 0.1$ $T_z = -2.5 \pm 0.1$	$A_i = 23.2 \pm 0.3$ $T_x = 6.0 \pm 0.3$ $T_y = -3.0 \pm 0.3$ $T_z = -3.0 \pm 0.3$	$A_i = 31.0 \pm 0.3$ $T_x = 4.4 \pm 0.3$ $T_y = -1.9 \pm 0.3$ $T_z = -2.5 \pm 0.3$
methylene	*g*	*g*	$A_i = -2.3 \pm 0.1$ $T_x = 4.4 \pm 0.1$ $T_y = -2.7 \pm 0.1$ $T_z = -1.7 \pm 0.1$	$A_i = 8.3 \pm 0.3$ $T_x = 6.0 \pm 0.3$ $T_y = -3.0 \pm 0.3$ $T_z = -3.0 \pm 0.3$	$A_i = 3.5 \pm 0.3$ $T_x = 4.4 \pm 0.3$ $T_y = -1.8 \pm 0.3$ $T_z = -2.5 \pm 0.3$

[a] Values are in megahertz. [b] This work. [c] Fassanella and Gordy.[13] [d] Hoganson et al.[9] [e] Warncke et al.[36] [f] Tommos et al.[4] [g] Not obtained.

nearby histidine. In this case, however, the proton is quickly released to some other basic residue; that is, the histidine acts as an immediate, but transient, proton acceptor. In a following step, the resulting tyrosyl radical receives from the OEC not only the electron but also the proton necessary to get back to the reduced Y_Z form. According to this model, Y_Z is therefore involved in an overall hydrogen atom abstraction process.

Our results obtained for the tyrosyl radical present in *N*-acetyl-L-tyrosine crystals have been compared with those obtained for Y_Z• and Y_D•. In Tables 4 and 5, we report also the results obtained for tyrosyl radicals in other systems.

The principal values of the tensors associated with ring protons are similar in all radicals, whereas the differences in the values of the tensors associated with the β protons are due to the different orientation of the methylene protons with respect to the ring plane (see Table 5).

Spin Densities. It has been suggested that the spin density distribution, and therefore the principal values of the hfc tensors, could be influenced by the environment surrounding the radical, mainly by the presence of a hydrogen-bond interaction in which the radical is the acceptor partner.[12] On the basis of crystallographic data,[21] one can state that the phenolic oxygen atom of *N*-acetyl-L-tyrosine is not involved in a hydrogen-bond interaction as an acceptor partner. In the previous paragraph, we have drawn the conclusion that the tyrosyl radical occupies in the crystal the same position as the undamaged molecule. Therefore, we can conclude that the tyrosyl oxygen atom is not involved in any hydrogen bond.

The comparison of literature data on hfc tensors for many different tyrosyl radicals, both hydrogen-bonded and non-hydrogen-bonded, and surrounded by different environments suggests that the spin density distribution remains almost constant and any external influence, if present, is weak. This is also consistent with recent ^{17}O measurements[8] and theoretical calculations.[36]

Dihedral Angles. In a previous paragraph, we have postulated that the value $B\rho^{\pi}_C$ in the McConnell relation for β protons is the same for the alkyl-substituted phenoxyl radicals, that is, $B\rho^{\pi}_C = 63$ MHz. Within this assumption, we have checked the values of the dihedral angle θ defined by the methylene group carbon−proton bond, C_1, and the normal to the ring reported in the literature for Y_D and Y_Z[4,5,35] (see Table 6). In other works,[4,35] the authors calculated the value of the two dihedral angles θ and $(120° - \theta)$ from the values of the measured isotropic hfc constants for the two β-protons using eq 1. The system of two equations gives θ and $B\rho^{\pi}_C$. The procedure followed by Rigby and co-workers[5] is slightly different but still needs the isotropic hfc constant for both methylene protons. Table 6 shows a very good consistency between the three methods. We point out that the knowledge of a correct value for $B\rho^{\pi}_C$ allows an evaluation of the dihedral angle even if only the isotropic hfc constant relative to a single methylene proton is measurable.

As a final remark, it is worth noticing that for the tyrosyl radical studied in this work the dihedral angles of the methylene protons are well-defined, unlike that for the tyrosyl radicals in photosynthetic RC and in glassy matrices. In fact, in the latter systems, there is a spread in dihedral angles that in the case of RC is due to small conformational differences and in frozen solutions is due to the glassy nature of the sample. In the present crystalline system, the radical has a unique conformation, as shown by the sharp ENDOR lines. The small difference between the ENDOR line width of the lines relative to the ring protons (~300 kHz) and the ones relative to the methylene protons (~500 kHz) can be explained by slightly different nuclear spin−spin relaxation times T_{2N} for the two types of proton.

In a recent work,[7] Hoff and co-workers using enantioselective 2H labeling have shown that Y_D• in PSII and the tyrosyl radical produced by UV irradiation in frozen solutions show, respectively, two different orientations of the phenoxyl ring relative to the two prochiral protons of the methylene group. In the present case, from the crystallographic data, it can be argued that the conformation of the undamaged molecule and therefore of the radical is the same as that for the tyrosyl radical in frozen solutions. Anyway, we point out that in the present case the

TABLE 6: Isotropic Hyperfine Coupling for Y_D• and Y_Z• and Corresponding Dihedral Angles Calculated in Different Systems[a]

	Y_D•				Y_Z•
	spinach (*S. oleracea*)[b]	*Chlamydomonas reinhardtii*[b]	*Phormidium laminosum*[b]	*Synechocystis* 6803[c]	*Synechocystis* 6803[d]
A^{β}_{H} meth. prot. 1 (MH_z)	28.6	30	26	23.1	31.0
A^{β}_{H} meth. prot. 2 (MHz)	6.3	5.7	8.1	8.3	3.5
θ_1[e]	48.1°[f]	47.2°[f]	50.7°[f]	52.0°[g]	44.0°[g]
θ_2[e]	72.1°[f]	72.7°[f]	69.3°[f]	68.0°[g]	76.0°[g]
$B\rho^{\pi}_{C}$ (MHz)[d]	64.1−66.7	65.0−64.4	64.8	60.9	59.9
θ_1[h]	47.6°	46.4°	50.0°	52.7°	45°
θ_2[h]	71.5°	72.5°	69.0°	68.7°	76.8°

[a] First and second rows: experimental values of isotropic hfc constant. Third to fifth rows: corresponding dihedral angles and $B\rho^{\pi}_{C}$ value. Last two rows: dihedral angles calculated with $B\rho^{\pi}_{C} = 63$ MHz. [a] Rigby et al.[5] [b] Warncke et al.[36] [c] Tommos et al.[4] [d] As reported elsewhere.[4,5,36] [e] Calculated with a best-fit method; see text. [f] Calculated with a two-equation system; see text. [g] This work.

TABLE 7: g Tensor Components in Tyrosyl Radicals in Different Systems

	N-ac-L-tyr[a] crystal (non-H-bonded)	L-tyr-HCl[b] crystal (H-bonded)	isolated PMP[c] calcd (non-H-bonded)	PMP−HAc[c] calcd (H-bonded)	RNR[d] *Escherichia coli* (non-H-bonded)	PSII Y_D•[e] *Synechocystis* 6803 (H-bonded)	PSII Y_Z•[e] *Synechocystis* 6803 (H-bonded)
g_x	2.0094 ± 0.0002	2.0067 ± 0.0005	2.0090	2.0066	2.00868 ± 0.00005	2.00740 ± 0.00005	2.00750 ± 0.00005
g_y	*f*	2.0045 ± 0.0005	2.0045	2.0042	2.00430 ± 0.0005	2.00425 ± 0.00005	2.00422 ± 0.00005
g_z	*f*	2.0023 ± 0.0005	2.0022	2.0021	2.00203 ± 0.00005	2.00205 ± 0.00005	2.00225 ± 0.00005
g_{iso}	2.0055 ± 0.0002	2.0045 ± 0.0005	2.0052	2.0044	2.00500 ± 0.00005	2.00466 ± 0.00005	2.00466 ± 0.00005

[a] This work. [b] Fassanella and Gordy.[13] [c] Un et al.[11] PMP means a para-methyl-phenoxyl radical. PMP−HAc means a molecule hydrogen-bonded with a CH_3COOH molecule. The relative orientation of the CH_3COOH molecule relative to the radical was taken from the structure of the diamagnetic L-tyr HCl structure. O···H distance = 1.59 Å. [d] Hoganson et al.[9] [e] Un et al.[33] [f] Not obtained.

conformation of the radical is governed by the intermolecular interactions in the molecular crystal, so that a comparison with tyrosyl radicals placed in proteic environment is not meaningful.

g *Tensor*. The presence of a hydrogen-bond interaction involving the tyrosyl radical as an acceptor partner has a big effect on the **g** tensor principal values. In fact, in phenoxyl radicals, the presence of such an interaction lowers the energy of the nonbonding orbitals of the oxygen atom and, therefore, enhances the difference in energy between these orbitals and the orbital where the unpaired electron is localized. As a consequence, on the basis of the theory of the **g** tensor,[11] the coupling between the ground state and those excited states where the electron is localized in a nonbonding orbital is lowered. Detailed calculations[11] predict that the g_x principal value (corresponding to the axis parallel to the C−O bond) should be particularly affected by the presence of a H-bond. According to the calculations, a value in the range $g_x = 2.0065-2.0090$ is expected depending on the strength of the H-bond, the minimum value corresponding to the strongest H-bond.

Our results are in agreement with these theoretical predictions. In fact, we have seen that the tyrosyl radical present in *N*-acetyl-L-tyrosine crystal is not involved in a hydrogen bond as an acceptor partner. In this situation, theoretical calculations predict a g_x principal value of 2.0090. The experimental value is 2.0094 ± 0.0002. Moreover, the comparison with the crystallographic directions has shown that the *x* axis is parallel to the C−O direction, as predicted theoretically.

An opposite situation has been found in a previous study on γ-irradiated L-tyrosine hydrochloride single crystals.[13] X-rays and neutron diffraction studies [37] have shown that in the undamaged crystal the phenolic oxygen is involved, as an acceptor partner, in a hydrogen-bond interaction. The donor partner is a COOH group of a neighboring molecule in the crystal.[39] The EPR results have shown that the phenoxyl radical produced by γ-irradiation is involved in the same kind of interaction.[13] The experimental value for g_x (2.0067 ± 0.0005) is very close to the theoretical value for a model system of a para-methylphenoxyl radical hydrogen-bonded to a CH_3COOH molecule.[11]

In Table 7, the **g** tensors for the tyrosyl radical we studied in *N*-acetyl-L-tyrosine single crystals and for different tyrosyl radicals[11,13,33,38] are reported.

It is worth noticing an important difference between these systems and the system studied in our work. *N*-Acetyl-L-tyrosine is a molecular solid, that is, charges are absent from the crystal structure. So, the radical studied in our work can be taken as a good model for a tyrosyl radical with the oxygen headgroup "free". On the other hand, L-tyrosine hydrochloride crystallizes in an ionic form. The presence of a Cl^- ion at 3.0 Å from the phenoxyl oxygen can strongly influence the energy levels of the radical and therefore can hide the pure effect of the presence of the hydrogen bond discussed above.

Conclusions

By performing ENDOR and HF-EPR experiments on a γ-irradiated single crystal of *N*-acetyl-L-tyrosine, we have carried out a detailed study on an oriented tyrosyl radical placed in an environment free from charge perturbations. The measurements of its magnetic properties can be helpful in the study of similar radicals found in biological systems, which are usually studied in disordered samples.

Acknowledgment. This work has been supported by CSSMRE of the Italian National Research Council and by EEC TMR contract FMRX-CT98-0214. The authors thank Prof. G. Zanotti and Drs. G. Valle and G. Agostini for help with the crystal growth and crystal structure, Dr. A. Di Matteo and Prof. M. G. Severin for helpful discussions, and Mrs. M. Zangirolami and S. Mattiolo for technical assistance.

References and Notes

(1) Debus, R. J.; Barry, B. A.; Babcock, G. T.; McIntosh, L. *Proc. Natl. Acad. Sci. U.S.A.* **1988**, *85*, 427.

(2) Barry, B. A.; Babcock, G. T. *Proc. Natl. Acad. Sci. U.S.A* **1987** *84*, 7099.

(3) Hoganson, C. W.; Lydakis Samantiris, N.; Tang, X. S.; Tommos, C.; Warnke, K.; Babcock, G. T.; Diner, B. A.; McCracken, J.; Styring, S. *Photosynth. Res.* **1995**, *46*, 177.

(4) Tommos, C.; Tang, X. S.; Warncke, K.; Hoganson, C. W.; Styring, S.; McCracken, J.; Diner, B. A.; Babcock, G. T. *J. Am. Chem. Soc.* **1995**, *117*, 10325.

(5) Rigby, S. E. J.; Nugent, J. H. A.; O'Malley, P. J. *Biochemistry* **1994**, *33*, 1734−1742.
(6) Hallahan, B. J.; Nugent, J. H. A.; Warden, J. T.; Evans, M. C. W. *Biochemistry* **1992**, *31*, 4562−4573.
(7) Niuwhenhuis, S. A. M.; Hulsebosch, R. J.; Raap, J.; Gast, P.; Lugtenborg, J.; Hoff, A. J. *J. Am. Chem. Soc.* **1998**, *120*, 829.
(8) Dole, F.; Diner, B. A.; Hoganson, C. W.; Babcock, G. T.; Britt, R. D. *J. Am. Chem. Soc.* **1997**, *119*, 11540.
(9) Hoganson, C. W.; Sahlin, M.; Sjöberg, B.-M.; Babcock, G. T. *J. Am. Chem. Soc.* **1996**, *118*, 4672.
(10) Smith, W. L.; Eling, T. E.; Kulmacz, R. J.; Marnett, L. J.; Tsai, A. L. *Biochemistry* **1992**, *31*, 3.
(11) Un, S.; Atta, M.; Fontcave, M.; Rutherford, A. W. *J. Am. Chem. Soc.* **1995**, *117*, 10713.
(12) Hoganson, C. W.; Babcock, G. T. *Biochemistry* **1992**, *31*, 11874.
(13) Fassanella, E. L.; Gordy, W. *Proc. Natl. Acad. Sci. U.S.A.* **1969**, *62*, 299.
(14) Box, H. C.; Budzinski, E. E.; Freund, H. G. *J. Chem. Phys.* **1974**, *61*, 2222.
(15) King, N. K.; Looney, F. D.; Winfield, M. E. *Biochim. Biophys. Acta* **1964**, *88*, 235.
(16) Hulsebosch, R. J.; van der Brink, J. S.; Nieuwenhuis, S. A. M.; Gast, P.; Raap, J.; Lungtenburg, J.; Hoff, A. J. *J. Am. Chem. Soc.* **1997**, *119*, 8685.
(17) Warncke, K.; McCracken, J. *J. Chem. Phys.* **1995**, *103*, 6829.
(18) Barry, B. A.; El-Deeb, M. K.; Sandusky, P. O.; Babcock, G. T. *J. Biol. Chem.* **1990**, *265*, 20139.
(19) Tomkiewicz, M.; McAlpine, R. D.; Cocivera, M. *Can. J. Chem.* **1972**, *50*, 3849.
(20) Sealy, R. C.; Harman, L.; West, P. R.; Mason, R. P. *J. Am. Chem. Soc.* **1985**, *107*, 3401.
(21) Koszlak, S. N.; van der Helm, D. *Acta Crystallogr.* **1981**, *B37*, 1122.
(22) Mueller, F.; Hopkins, M. A.; Coron, N.; Grynberg, M.; Brunel, M. C.; Martinez, G. *Rev. Sci. Instr.* **1989**, *60*, 3681.
(23) Atherton, N. M. *Principles of Electron Spin Resonance;* Ellis Horwood: London, 1993.
(24) McConnell, H. C.; Strathdee, J. *Mol. Phys.* **1959**, *2*, 129.
(25) Qin, Y.; Wheeler, R. A. *J. Am. Chem. Soc.* **1995**, *117*, 6083.
(26) Himo, F.; Gräslund, A.; Eriksson, L. A. *Biophys. J.* **1997**, *72*, 1556.
(27) Adamo, C.; Subra, R.; Di Matteo, A.; Barone, V. *J. Chem. Phys.* **1998**, *109*, 10244.
(28) Brustolon, M.; Maniero, A. L.; Bonora, M.; Segre, U. *Appl. Magn. Reson.* **1996**, *11*, 99.
(29) Drew, R. C.; Gordy, W. *Radiat. Res.* **1963**, *18*, 552.
(30) Liming, F. G.; Gordy, W. *Proc. Natl. Acad. Sci. U.S.A.* **1968**, *60*, 794.
(31) Nordio, P. L.; Pavan, M. V.; Giacometti, G. *Theor. Chim. Acta* **1963**, *1*, 302. Corvaja, C.; Giacometti, G. *Theor. Chim. Acta* **1969**, *14*, 352.
(32) Box, H. C. *Radiation Effects: ESR and ENDOR Analysis;* Academic Press: New York, 1977.
(33) Un, S.; Tang, X. S.; Diner, B. A. *Biochemistry* **1996**, *35*, 679.
(34) Force, D. A.; Randall, D. W.; Britt, R. D.; Tang, X. S.; Diner B. A. *J. Am. Chem. Soc.* **1995**, *117*, 12643.
(35) Tang, X. S.; Zheng, M.; Chisholm, D. A.; Dismukes, G. C.; Diner B. A. *Biochemistry* **1996**, *35*, 1475.
(36) Warncke, K.; Babcock, G. T.; McCracken, J. *J. Am. Chem. Soc.* **1994**, *116*, 7332.
(37) Gilchrist, M. L., Jr.; Ball, J. A.; Randall, D. W.; Britt R. D. *Proc. Natl. Acad. Sci. U.S.A.* **1995**, *92*, 9545.
(38) O'Malley, P. J.; Ellson, D. *Biochim. Biophys. Acta* **1997**, *1320*, 65.
(39) Frey, M. N.; Koetzle, T. F.; Lehmann, M. S.; Hamilton, W. C. *J. Chem. Phys.* **1973**, *58*, 2547.
(40) Gerfen, G. F.; Bellen, B. F.; Un, S.; Bollinger, J. M.; Stubbe, J.; Griffin, R. G.; Singel, D. J. *J. Am. Chem. Soc.* **1993**, *115*, 6420.